Japan Journal of Research

Original Article

Statistical Analysis of Visible and Infrared Radiation in The Museum of L'Almoina in Valencia (Spain)

Juan-Carlos Moreno[1], José Luis Baró[2], María-Antonia Serrano[3], Fernando-Juan García-Diego[1*]

[1]Department Applied Physics, Universitat Politècnica de València, Camino de Vera, s/n, 46022 Valencia, Spain
[2]Department of Architectural Composition, Universitat Politècnica de València, Camino de Vera, s/n, 46022 Valencia, Spain
[3]Biomaterials and Tissue Engineering, Universitat Politècnica de València, Camino de Vera, s/n, 46022 Valencia, Spain

Correspondence

Juan-Carlos Moreno
Department Applied Physics, Universitat Politècnica de València, Camino de Vera, s/n, 46022 Valencia, Spain

E-mail: jcmestev@fis.upv.es

Tel: +34-9638-77000 (ext. 75241)

Abstract

The present work is an analysis and statistical association of distributions of experimental spectral values of visible and infrared radiation attenuation through the skylight of a museum in the city of Valencia (Spain). They have been statistically analyzed in summer and winter. This analysis allows detecting interrelation between data distributions. The spatial association of these distributions is also analyzed by applying the Yule index belonging to Spatial Statistics. The interest of the index is to establish a relationship of spatial association of distributions and the structure of the museum. That is, a contingency matrix is constructed whose value of the elements depends on the shape of the museum's skylight.

- Received Date: 12 Dec 2022
- Accepted Date: 20 Dec 2022
- Publication Date: 02 Jan 2023

Introduction

It is well known that prevention and maintenance of archaeological monuments is necessary. This is known the requirements are collected in the international charters on the protection of archaeological sites [1-5].

One of the parameters to define is the effect of light radiation on archaeological materials. In [6] the effects of pigmentation change by light radiation are studied.

In this work, the effects of visible and infrared radiation are analyzed. The aim of analysis is a museum built in 2006 in Valencia (Spain), to preserve an archaeological site dating back to the founding of the city in the Roman Republican era [7, 8]. As cover of that museum, 300 m2) skylight roof was built. The skylight collects more light and offers a very striking transparency effect to the public. In its constitution it consists of a glass plate with three sheets, with a thin layer of water on top, which exerts a projecting undulation inside the museum [9].

In contrast to such a positive visual effect, the skylight entails cleaning maintenance, repair of leaks and formation of efflorescence [10]; as well as an increase in microorganisms, vegetation, insects and the greenhouse effect with the consequent low energy effectiveness [11].

Natural lighting inside the museum produces great contrasts in the area directly below the skylight and the surrounding areas hidden by opaque surfaces.

To solve the problems, it was proposed to transform the structure into a pyramidal one [12], or to eliminate the layer of water [13]. This decision was made to maintain the original structure [14], since the elimination of the water layer makes thermal control impossible [15,16].

The pernicious effect of transparent protections has been observed in places with archaeological heritage. In example, the Roman Palace of Fishbourne in West Sussex (England) and the Villa Romana of Piazza Armerina in Sicily (Italy).

F.Yaka [17] studied the advantages and disadvantages of transparent protection, concluding that it is necessary to carefully select the material based on the thermophysical properties. Michalsky [6,18,19], has recommended a combination of lighting and low impact on the objects for the sake of their conservation.

Horie [20], proposed the use of solar control films to reduce levels of sunlight without making changes to the structure. Al-Obaidi et al. [21] detected in glass in museum skylights, about the need to control UV rays. Other authors [22–25], have proposed glass filters the UVB band of solar radiation but transmits a large part of the UVA band.

Tuchinda et al. [25], came to the conclusión that clear glass allows up to 72% of UV light and up to 90% of VIS to pass through, depending on the thickness of the glass.

Li et al. [26] studied circumstances that influence the UV protection properties of glass.

Citation: Juan-Carlos M, José Luis B; María-Antonia S; Fernando-Juan G-D. Statistical Analysis of Visible and Infrared Radiation in The Museum of L'Almoina in Valencia (Spain). Japan J Res. 2023;4(1):1-9

***Figure 1**. (a) Exterior of the "Museo de l'Almoina"; (b) interior of the museum just below the skylight.*

For example, type of glass, color, design and coating. The decrease in transmittance was analyzed as the thickness of the glazing sheets increased. Transmittance spectra were measured, showing small differences between different film thicknesses in the VIS range and a large difference in the UV and NIR bands.

Serrano and Moreno [27] studied the spectral transmission of solar radiation from different translucent materials. They showed that smoked glass has a transmittance between 56 and 68% in the UVB band and 70% in the UVA band. In the smoked glass, lower transmittances were obtained as the temperature was higher, being the origin of this fact in the reduction of the thermal conductivity when the temperature increases [28].

Long et al. [29], they studied the performance of thermochromic double glazing in building application, and Aguilar el al. [30] analyzed the effect of double glazing in concrete in a market.

In this work, the term "relative attenuation" (RA) as the relationship between the incident external radiation and the emerging radiation of the skylight, being a concept not included in the heritage conservation regulations [31,32].

The objective of this work is to analyze the spectral solar radiation that passes through a skylight of an archaeological museum. Such skylight contains a thin layer of water in its upper part. Spectral solar radiation was measured (visible (VIS) and infrared (IR) bands at specific points in the museum (north, west, east and center of the skylight) and spectral attenuation was determined. This magnitude allows comparisons between points. Spectral measurements allow the detection of changes or disturbances in specific areas of the spectral bands. While global values are important, they do not help to understand specific behaviors, and in the case at hand, structures that partially block light, more information is obtained with attenuation of spectral radiation

First, a basic statistical analysis of the attenuations calculated from the experimental data is performed. This provides a global view of the evolution of the data as a result of the presence of the museum's skylight. Secondly, an exploratory data analysis is carried out following the ideas of Tukey [33]. Third, notions of spatial statistics apply to detect associations between data distributions. As common concepts, the following works stand out: the elaboration of the so-called contingency matrices, and the use of the $\chi 2$ test using Croxton's formula [34], as duly explained in the Methodology section. Another more direct method is the use of "association degree indices", such as the "Q index" (or Yule index) (Gifford and Kroeber, [35]) (Kluckhohn,[36]), and the "V index" (Milke,[37]; Driver [38]. Since the Q index equation is the simplest, it has been adopted in this work.

Solar radiation were measured in three bands: UV (300-400 nm), Visible (400-700 nm) and Near Infrared, depending on the interval (700-900 nm), (published in Serrano el al.[39]), and the following tasks have been carried out in this work: Analysis of visible and infrared values; evolution of the spectral radiation for each measurement point in the museum; the comparison between series of measurements (between interior points in the summer). Determining associations of data distributions using the Q index. Because we have a continuous Q-index equation, we can apply differential calculus and determine the total differential and rates of change, as well as determine a spectral Q- index. Ultimately the origin of the variations is due to the configuration of the museum.

Materials and methods

Tested materials

The experimental measurements were carried out in the Museo de l'Almoina, located in the historic center of Valencia (Spain); coordinates 39º 28' N, 0º 22' W; at the sea level. The study focused on a skylight made of laminated glass that is made up of three sheets of glass 10 mm thick joined by sheets of polyvinyl butyral (PVB) (Figure 2), whose function is to increase the bending resistance of the glass, according to the adhesion capacity of the sheets, guaranteeing safety against breakage. It also contributes to reducing the relative attenuation of visible and infrared radiation, as verified in this work.

Spectral measuring devices

Spectral irradiances were measured with an Ocean Optics spectrometer [40]: HR4000 for visible and infrared radiation in the range of 400 nm to 1100 nm. The measurement points were outside and at different points inside the museum, subsequently determining the relative attenuations.

The HR4000 schematic is indicated in Figure 3. The electromagnetic radiation passes through a fiber optic cable to the spectroradiometer. A key element in the transmission is an SMA connector. The regulation of the amount of light is carried out with a slit which falls on the optical bench. A reflection of the radiation occurs in a collimator-type mirror, producing diffraction. In a next stage it is projected to the charge coupled device (CCD) which converts the optical signal into digital. Finally the information is transmitted from a USB port to the computer and will be processed by relevant software.

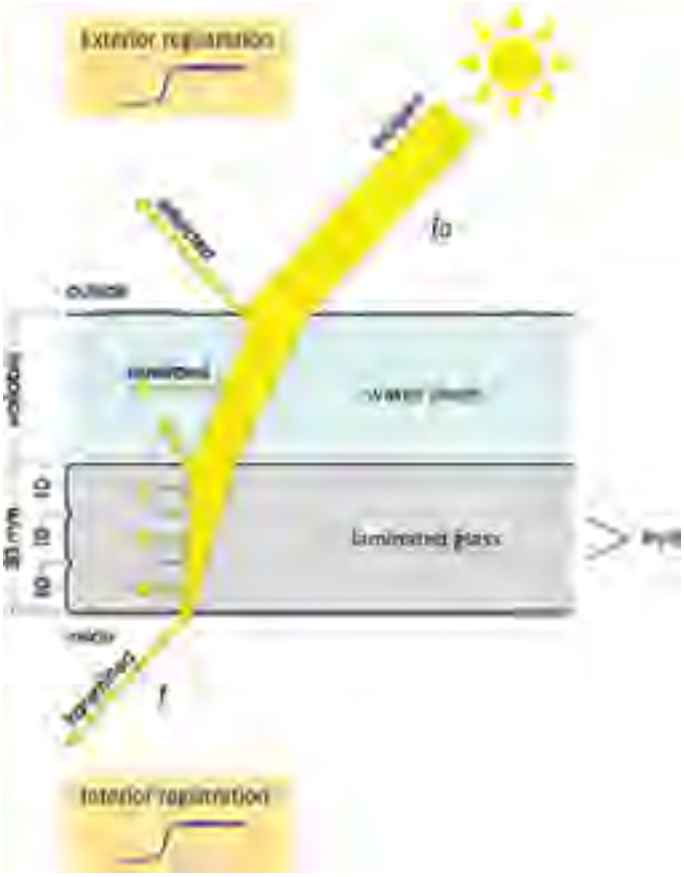

Figure 2. *Light intensity attenuation through the skylight the skylight and the water layer. The initial intensity is represented by "Io" so that it is reduced by the partial absorption and reflection that occurs circulating through the different layers, reaching the transmission of a fraction to the interior "I".*

Figure 3. *Operating diagram of an optical spectrometer such as the one used in this study [41].*

Table 1. *Specifications of spectrometer used [42].*

Ocean Insight	FLAME-S-UV-VIS
Detector	Linear silicon CCD array
Entrance slit	25 µm
Grating	#1
Pixels	2048
Integration time	1 ms–65 s
Optical resolution	1.33 nm FWHM (typical)
Wavelength range	200–850 nm
Input fibre connector	SMA 905
Signal-to-noise ratio	250:1 (full signal)
Stray light	<0.10% at 435 nm
Calibration uncertainty	10%
Wavelength step	0.10 nm

Figure 4. *Spatial distribution of studied points. East point (E), Central point of the skylight (C), North point (N), and West point (W).*

The spectrometer was calibrated in July 2017 from 250 to 400, by Ocean Optics, with a measurement uncertainty of approximately 10% across the entire measurement spectrum.

To cover the objective of this work, was distributed the visible range (VIS) [400, 700] nm and for infrared, [700, 1100] nm.

Data collection

The task of receiving the information provided by the spectroradiometer was performed on a conventional PC using SpectraSuite from Ocean Optics, suitable for HR4000-VIS- NIR.

The stages of realization were the following: 1º.- Outside the museum, the sensor was placed so that it captured the point of maximum light intensity, that is, towards the solar position such that the normal spectral solar irradiance was recorded. 2º.- Immediately afterwards, measurements were made at 4 points just below the projection of the skylight (Figure 4). 3º.- The measures were repeated to avoid possible errors.

The four measurement points were "E" to the East, just at the entrance; point "N" north of the museum, where there is a corridor; "W" on west side of skylight; and point "C", in the central point of the museum under the skylight.

Two days of measurements were carried out throughout the year: one in winter (14 January 2020) and one in summer (30 July 2019). At the top of the skylight there is a thin layer of water (3 cm). In those days it was measured at different times of the day: morning (9:00 AM), noon (12:00 PM) and afternoon (3:00 PM) (solar time) and forever the spectral values were taken were clear. The solar zenith angle on the data collection days is shown in Table 2.

This procedure was repeated on different days Table 2. Solar zenith angle (SZA), in degrees, for the studied periods.

Table 2. *Solar zenith angle (SZA), in degrees, for the studied periods.*

	Morning	Noon	Afternoon
30/07/2019	44.84	19.94	41.80
14/01/2020	75.32	60.97	72.74

Calculation of relative attenuation

When light reaches a semi-transparent surface, part of it is reflected, part of it is absorbed and part of it is transmitted through the object (Figure 1). This phenomenon can be expressed by the following irradiance balance that can be particularized for each wavelength:

$$\text{Irrad}_{incident,\lambda} = \text{Irrad}_{reflected,\lambda} + \text{Irrad}_{absorbed,\lambda} + \text{Irrad}_{transmitted,\lambda} \quad (1)$$

Optical relative attenuation, as the main magnitude on which this entire study pivots, defines a relative (dimensionless) quantity that measures the fraction of incident light passing through a sample, in this case, the glass of the skylight. It is expressed by the result of dividing the transmitted light maximum intensity (I_{max}) by the incident maximum ray intensity ($I_{0,max}$).

$$RA = I_{max} / I_{0,max} \quad (2)$$

The calculations for obtaining this relative attenuation values were based on the data provided by the spectrometer oriented to the maximum intensity of light (I_{max}, $I_{0,max}$) for each transmitted wavelength.

Comparative relative attenuations

The relative attenuation calculations were compared at different times (9:00 AM, 12:00 PM and 3:00 PM solar hours) for the same season and same points to evaluate the influence of irradiance due to the different orientations and inclinations of the sun throughout the day.

The spectral values of all the points recorded by the VIS and NIR bands were considered for the same season, the same time and the same skylight situation (clear days without clouds) to take into account the spatial variations in relative attenuation inside the museum.

The selected data were arranged in tables and presented in graphs using Microsoft Office Excel for a clear visualization of the results.

Statistical study

In the first place, the basic descriptive statistics are carried out using the statistics: mean, standard deviation and coefficient of variation, which are useful to establish the comparison of measurements and the detection of data dispersion taking the central value as a reference. In this case we are interested in determining the grouping of radiation attenuations within the interval [0 , 1], which corresponds at the unit end to a radiation equal to the central point C where the maximum luminosity falls.

To analyze the association between the data distributions at the interior points of the skylight, taking into account the existence of factors that control and determine a pattern, they almost always affect more than one distribution. A tool that helps achieve this purpose is Association Analysis [35]. It consists first in the construction of the contingency matrix, which contains in the rows the frequencies of the values obtained in the arbitrary partition of the data, using the interval [0 , 1] nm; and the number of partitions of said interval is arbitrary, using [0, 0.5] nm and [0.5001, 1] nm. The proposed partition is placed both in a row and in a column, resulting in a square matrix (Table 3).

In this case, the variables mentioned correspond to the VIS radiation attenuation intervals at the measurement points.

Table 3. *Contingency matrix for two variables.*

	DISTRIBUTION TYPE A	
DISTRIBUTION TYPE B	a	b
	c	d

The cells of the matrix represent the covariation of the ranges of the variables, with cell "a" meaning the joint presence of the values of the two distributions in the first range; cell "b" represents the joint presence of the values of the first range of distribution B and the values of the second range of distribution A; cell "c" is the presence of values in range two of distribution B with values in range one of distribution A; cell "d" is the covariation of the elements of the two distributions belonging to rank two.

The Q index is defined as,

$$Q = \frac{ad - bc}{ad + bc} \qquad (3)$$

TThe interval of existence of the index is [-1 , +1], being the value (+1) the maximum positive association, and the value (-1) the maximum negative association, which corresponds to the segregation between distributions. The null value occurs when there is no evidence of association.

The values of the Q index are related to the structure of the museum, since the interdependent values (a, b, c, d of equation 3) are directly proportional to the geometric shape of the premises."

Results

Relative variations of the visible attenuation between interior points of the museum in summer and winter

As detailed in the Methodology section, the radiation attenuations of three points inside the museum are compared. The relative variation of the visible attenuation of the interior points (east (E), north (N) and west (O)) is studied, taking as reference a central point (C) of the skylight (see figure 4). The south point is omitted because the results are symmetric with the north point. The results are shown in table 4.

Table 4. *Determination of the relative attenuation of the visible radiation of the measurement points with respect to the central point considered as reference.*

	Point /reference	Average	Standard-deviation	Coef. Variation
WINTER	East / central	0,84	0,13	15%
	North / central	0,82	0,13	16%
	West / central	0,52	0,11	21%
SUMMER	East / central	0,95	0,02	2%
	North / central	0,98	0,01	1%
	West / central	0,28	0,04	14%

At measurement point W, the relative attenuation is lower than at the other points because there is a greater number of hours of sunshine, and furthermore, specifically in summer, the intensity of incident solar radiation is much higher. However, the increase in radiation produces a greater number of interferences and therefore a greater coefficient of variation.

Relative variations of the infrared attenuation between interior points of the museum in summer and winter

Similarly, this paragraph studies the infrared radiation attenuations of three points inside the museum. It is considered that the relative variation of infrared attenuation of the interior points (east (E), north (N) and west (W)) is analyzed, taking a central point (C) of the skylight as a reference (see figure 4) . The south point is omitted because the results are symmetric with the north point. The results are shown in table 5

Table 5. *Determination of the relative attenuation of the visible radiation of the measurement points with respect to the central point considered as reference.*

	Point /reference	Average	Standard-deviation	Coef. Variation
WINTER	East / central	0,84	0,13	15 %
	North / central	0,82	0,13	16%
	West / central	0,52	0,11	21%
SUMMER	East / central	0,95	0,02	2%
	North / central	0,98	0,01	1%
	West / central	0,28	0,04	14%

By means of the coefficient of variation, it is deduced that there is a great dispersion of the relative attenuations, since in this area of the spectrum, a greater number of influences from the environment itself are produced. Reflections and refractions are very different from the visible region because the refractive index varies with wavelength (Cauchy's equation [43]). In the infrared region the refractive indices can be considerably higher. It highlights the fact that the relative attenuation at point W is lower than the other points, being the same cause mentioned in the visible region.

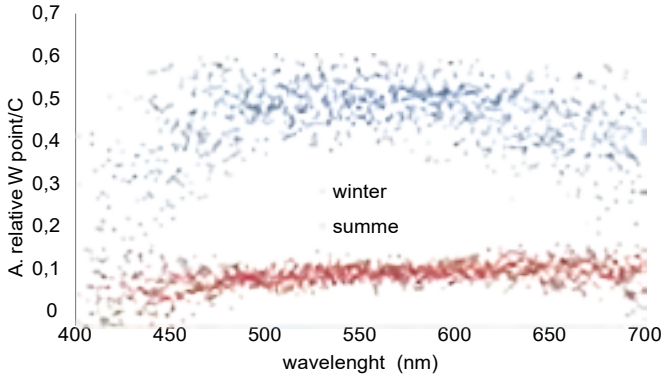

Figure 5. *Spectral relative attenuation between points W and C. Visible region.*

As an example of the distribution of the relative spectral attenuation points, Figure 5 shows the comparison of the west point of the skylight in winter and summer of the visible region, always taking the central point as a reference.

It is observed that in summer, the relative attenuation is very small as a result of the high intensity of solar radiation and the high number of hours of sunshine. The skylight also behaves a little differently in winter, since the evolution of the relative attenuation changes at the extremes of the visible region, with respect to the center of said region (550 nm).

Figure 6 shows the comparison of the west point of the skylight in winter and summer in the infrared region, always taking the central point as a reference.

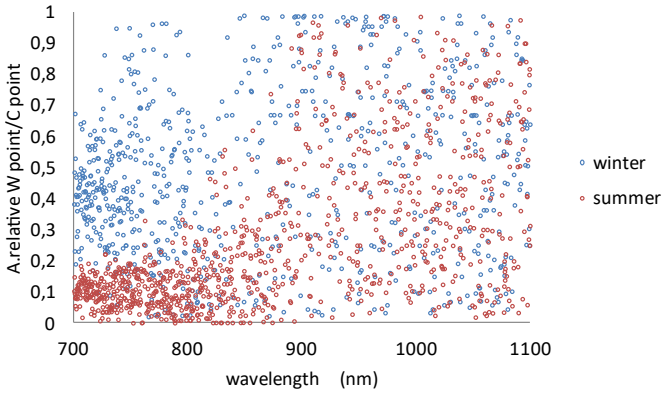

Figure 6. *Spectral relative attenuation between points W and C. Infrared region.*

A high dispersion of the values in the IR zone is shown. Between 700 and 800 nm there is a certain concentration of points at two levels of attenuation (0.4 in winter and 0.1 in summer); beyond 800 nm a scattered and random distribution occurs for the winter and summer points. The reason has already been discussed in Table 5.

Variations of the visible and infrared attenuation of the central point of the museum in summer.

This section studies the attenuation of solar radiation at the central point of the museum at different times of a summer day. Summer has been chosen because the solar radiation is higher and the measurements show less dispersion when the attenuation is determined, since the sun's rays have a more perpendicular incidence orientation in the skylight. On the contrary, in winter, the solar radiation has a greater inclination, the diffuse component incident on the skylight being greater than in summer, and this has a greater dispersion as a consequence. Figure 7 shows the attenuation at three different times (9:00 AM; 12 PM; 3:00 PM) in the visible region. At 12:00 pm. the dimming is less, except at the near-infrared end, where it is the 9:00 A.M. minor. The skylight filters less radiation when the incident radiation is more intense. At 3:00 pm. the attenuation of this distribution of points is, in the entire visible region, greater than the other two.

Figure 8 shows the attenuation at three different times (9:00 AM; 12 PM; 3:00 PM) in the infrared region. The greatest attenuation occurs in the afternoon distribution. And the minor, with the distribution of points in the morning. The figure shows a high dispersion, in all point distributions, from 900 nm, reaching a random relationship, its origin being in the behavior of the skylight materials. Recall the comment in table 6.

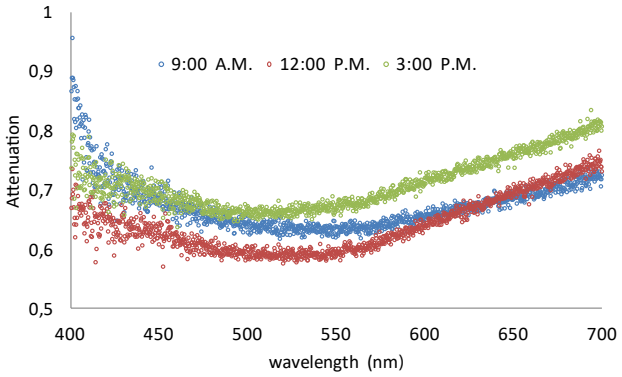

Figure 7. *Spectral attenuation at center point C. Visible region.*

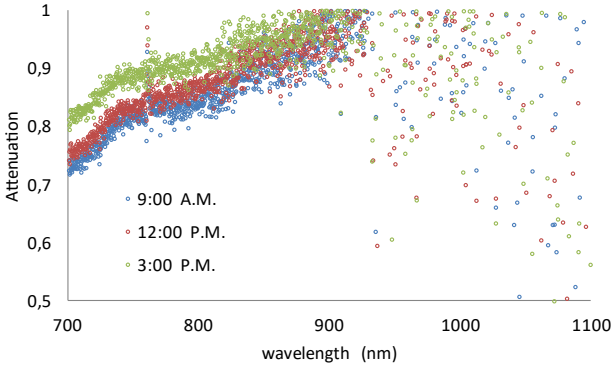

Figure 8. *Spectral attenuation at center point C. Infrared region.*

Analysis of association between distributions of measures

The association of distributions contributes to the knowledge of the behavior pattern of the museum installation. The geometric shape contributes to the path of electromagnetic radiation in its interior, producing a specific distribution that can present convergences with another distribution made at another moment

or separated in space and simultaneously. The Q index described in the methodology represents a measure of the possible association between distributions. Table 6 shows the association results of relative attenuations (in the visible and infrared regions) between inland points in summer. The most interesting points to compare are the museum entrance (East) with the north, since both are located indoors (much more pronounced in the north point), and the East point with the West since they belong to the evolutionary curve of the Sun.

Table 6. *Q index values between the North, West and East measurement points, for both visible and infrared radiation.*

	Point North		Point West	
	VIS	NIR	VIS	NIR
Point East	-0,5	-0,004	-0,33	-0,085

The fact in the infrared zone that there is no association stands out (virtually zero values). In the visible area, there is a more pronounced segregation of the distributions between the North and East distributions, the reason for which has been commented on in the previous paragraph.

For another form of museum building, it will produce another value of such contingency table which, in turn, leads to the Q index. To evaluate hypothetical changes in increase or decrease, we proceed with the determination of the differential of equation (3); in this way, the variation of the Q index with respect to the values of the contingency matrix (a,b,c,d) is obtained. The parts of the differential of Q are:

$$\left(\frac{\partial Q}{\partial a}\right)_{b,c,d} = \frac{d[1-Q]}{ad+bc} \qquad (4)$$

$$\left(\frac{\partial Q}{\partial a}\right)_{a,c,d} = \frac{-c[1+Q]}{ad+bc} \qquad (5)$$

$$\left(\frac{\partial Q}{\partial c}\right)_{a,b,d} = \frac{-b[1+Q]}{ad+bc} \qquad (6)$$

$$\left(\frac{\partial Q}{\partial d}\right)_{a,b,c} = \frac{-a[1-Q]}{ad+bc} \qquad (7)$$

The utility of differentiation is twofold; On the one hand, it is used to predict changes in the Q index when the elements of the contingency matrix (a,b,c,d) vary. That is, if we assume a different skylight museum structure, it will produce modified matrix elements (for example, for Q = 0.5 and a = 5; b = 0; c = 0; d = 1; and for simplicity a differential variation of matrix elements equal to 0.1), leads to a total differential, dQ = 0.02; being for the example, Q ± dQ ; (0.5 ± 0.02).

On the other hand, the partial derivatives (eqs. (4) to (7)) indicate the speed of variation of the Q index with respect to the value changes in the cells of the contingency matrix. Each cell represents the intersection of values, grouped into ranges, between two distributions. A continuous global museum structure will imply a high association of values since they receive the same external interactions, which in this work is solar radiation and studied through its attenuation. Saying that they present an association is similar to manifesting the same behavior. If the structure of the building presents separation compartments inside, as is the case of the L'Alomina museum where the East and North points are under cover and the West point is uncovered, the interactions from the outside are not the same, and that implies a negative association between the values. For this reason, in Table 6, negative results appear. For example, for the index Q between the North and East points, whose value is -0.5, it comes from the following values of the elements of the contingency matrix: a = 69; b=245; c=1085; d = 1261. Then, substituting in equations 4 to 7, the velocities are obtained,

$$\left(\frac{\partial Q}{\partial a}\right)_{b,c,d} = 5,36\cdot10^{-3}; \quad \left(\frac{\partial Q}{\partial a}\right)_{a,c,d} = 1,53\cdot10^{-3};$$

$$\left(\frac{\partial Q}{\partial c}\right)_{a,b,d} = -3,47\cdot10^{-3}; \quad \left(\frac{\partial Q}{\partial d}\right)_{a,b,c} = -2,93\cdot10^{-3}$$

Where it is observed that the positive evolution of Q occurs only when the value of "a" of the contingency matrix increases. This value represents intersection of small values of attenuation between the two distributions. However, when the rest of the elements of the matrix (b, c, d) increase, they produce a decrease in the Q index, that is, it harms the association of high attenuation values between the distributions. It highlights the fact that the influence exerted by the value "c" is the greatest among all.

This analysis opens expectations of predicting the behavior of a construction according to its geometry. If certain characteristics regarding the configuration of the museum lead to specific values of the Q index, then the inverse path can also be achieved since it is a continuous relationship, that is, finding an equation or equations that taking as parameter the Q index, can predict stereospatial configurations of the museum. It will be objective in the next job.

Q Spectral Index

It is well known that electromagnetic propagation through materials undergoes various phenomena such as reflection, refraction, absorption, polarization, etc., and all of them have a strong dependence on wavelength, because the behavior of materials during the transit. In addition, the stereospatial arrangement of these materials also influences. So ultimately, the Q index will be influenced by the wavelengths that are in play.

In this section, a spectral function of the Q index is deduced from the experimental measurements carried out in the museum. Starting from two distributions of points, for example, for the visible region, comparison of relative attenuations of the East and North points of the summer museum at noon are made. Q indices are evaluated by wavelength bands, covering the visible region [400, 700] nm. The result is shown in Figure 9, from which it can be deduced that there is no association between these two distributions of points in the area of the visible region close to ultraviolet; however, strong association occurs at wavelengths between 475-540 nm. (cyan and green colors). Starting from the yellow color, the association of the points decreases to zero up to 700 nm.

It is noteworthy that the maximum of the curve in figure 9 coincides with the maximum intensity of incident solar radiation (range 500 to 550 nm). It is possible that the incident radiation of greater intensity is distributed more uniformly inside the museum, and exerts a common effect in a greater number of points, hence it is translated with a specific value of the association parameter Q.

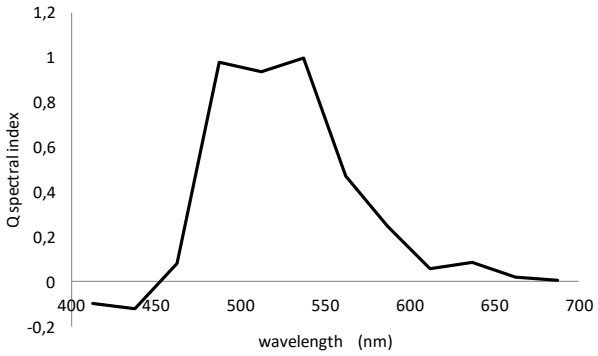

Figure 9. *Q index as a function of wavelength between relative attenuations of the East and North points, (summer at 12 P.M.).*

Discussion

As a conclusion of this work, the following comments can be made. At measurement point W, the intensity of incident solar radiation is much higher. The increase in radiation produces a greater coefficient of variation.

In the infrared region the greatest attenuation occurs in the afternoon distribution, and the minor, with the distribution of points in the morning. Its origin is the dependence of the refractive index on the wavelength.

Through differentiation is analized the positive evolution of Q. Occurs only when the value of "a" of the contingency matrix increases. But, when the rest of the elements of the matrix (b, c, d) increase, they produce a decrease in the Q index. It highlights the fact that the influence exerted by the value "c" is the greatest among all.

Also, the differentiation is used to predict changes in the Q index when the elements of the contingency matrix (a,b,c,d) vary. The partial derivatives (eqs. (4) to (7)) allow to evaluate the speed of variation of the Q index with respect to the value changes in the cells of the contingency matrix. Saying that they present an association is similar to manifesting the same behavior. If the structure of the building presents separation compartments inside the interactions from the outside are not the same, and that implies a negative association between the values. It is an objective for future works to parameterize the configuration of a museum through the Q index.

Another innovative point of this work is the determination of the Q index as a function of the incident radiation wavelength. A similarity of shape is found between the solar radiation intensity curve and the spectral Q index dependence curve.

Author contributions

J.-C.M.E., conceptualization, methodology, formal analysis, writing—original draft, preparation, writing—review and editing. M.-A.S., conceptualization, methodology, formal analysis, writing—original draft, preparation, writing—review and editing. J.-L.B.Z., formal analysis, writing— original draft, preparation, writing—review and editing. F.-J.G.-D., formal analysis, preparation, writing— review and editing, funding acquisition. All authors have read and agreed to the published version of the manuscript.

Funding

This research was funded by the European Union's Horizon 2020 research and innovation program under grant agreement No. 814624.

Institutional review board statement

Not applicable

Informed consent statement

Not applicable.

Author contributions

The authors are grateful to the "Ajuntament de València" and to Vicent Escrivà Torres, director of the "l'Almoina" museum, for their assistance and authorization of the data collection to carry out this work.

Conflicts of interest

The authors declare no conflict of interest. The funders had no role in the design of the study; in the collection, analyses, or interpretation of data; in the writing of the manuscript, or in the decision to publish the results.

References

1. Committee for drafting the International Charter for the Conservation and Restoration of Monuments. International Charter for the conservation and restoration of monuments and sites (The Venice Charter). In 2nd International Congress of Architects and Technicians of Historic Monuments, 1964; art. 14.
2. International Committee for the Management of Archaeological Heritage (ICAHM). Charter for the Protection and Management of the Archaeological Heritage (Icomos Charter); 1990; art. 6.
3. Commission Internationale de L'éclairage. Control of Damage to Museum Objects by Optical Radiation; Fer: Vienna, Austria, CIE 157:2004 Division 3 ISBN: 9783901906275
4. Conservación del Patrimonio Cultural. Especificaciones para el Emplazamiento, Construcción y Modificación de Edificios o Salas Destinadas al Almacenamiento o Utilización de Colecciones del Patrimonio. UNE-EN 16893:2019. Asociación Española de Normalización (UNE), Madrid; 2019.
5. Camuffo, D. Chapter 4. Radiation and Light. Conservation, Restoration, and Maintenance of Indoor and Outdoor Monuments. In Microclimate for Cultural Heritage; Elsevier: Amsterdam, The Netherlands, 2014; pp. 131–164.
6. Michalski, S. Light, ultraviolet and infrared. In Agent of Deterioration: Light, Ultraviolet and Infrared; Available online: https://www.canada.ca/en/conservation- institute/services/agents-deterioration/light.html (accessed on 08 April 2022).
7. Ribera, A. El centro Arqueológico de l'Almoina. Valencia. In Proceedings of the 5. Encuentro Internacional. Actualidad en Museografía, Palencia, Spain, 1-3 Octuber 2009; pp. 67–82.
8. Ribera i Lacomba, A. El centro arqueológico de l'Almoina en Valencia. In Archeologia e Città: Riflessione Sulla Varizzazione dei Siti archeologici in Aree Urbane; Ministero dei Beni e delle Attività Culturali e del Turismo. Soprintendenza Speciale per i Beni Archeologici di Roma, Palombi editore; 2012; pp. 37-45; ISBN 978-88-6060-600-6.
9. Herrera García, J.M.; Rueda Muñoz de San Pedro, J.M. Memoria del "Proyecto de Ejecución para las Obras de Cimentación, Estructura y Cubierta Mediante Plaza Pública de los Restos Arqueológicos de l'Almoina de Valencia; Unpublished; 2002. Available online: https://dogv.gva.es/datos/2001/11/29/pdf/2001_M11450.pdf (accessed on 08 April 2022).
10. Pérez Ema, N. Degradación del material pétreo en yacimientos arqueológicos. Rev. electrónica ReCoPar 2016, 11, 39–58. Available online: https://www.semanticscholar.org/paper/Degradaci%C3%B3n-del-material- p%C3%A9treo-en-yacimientos- Ema/ac1b2823ae9d28c255649622c9d4d80ec549e5f7?p2df (accessed on 08 April 2022).

11. Padfield, T. How to Keep for a While What You Want to Keep forever; Available online: https://www.conservationphysics.org/phdk/phdk_tp.html (accessed on 08 April 2022).
12. García, H. El Estanque de la Plaza de la Almoina se Sustituirá por un Lucernario Piramidal; Available online: https://www.levante- emv.com/valencia/2013/05/19/estanque-plaza-almoina-sustituira-lucernario- 12896876.html (accessed on 08 April 2022).
13. Moreno, P. El Centro Arqueológico de la Almoina de Valencia se Reformará a los once Años de su Apertura. Available online: https://www.lasprovincias.es/valencia- ciudad/ayuntamiento-encarga-estudio-almoina-20181024131618-nt.html (accessed on 08 April 2022).
14. Fernández-Navajas, Á.; Merello, P.; Beltrán, P.; García-Diego, F. Multivariate thermo-hygrometric characterisation of the archaeological site of Plaza de l'Almoina (Valencia, Spain) for preventive conservation. Sensors 2013, 13, 9729– 9746.
15. Merello, P.; Fernández Navajas, Á.; Curiel-Esparza, J.; Zarzo, M.; García-Diego, F.J. Characterisation of thermo-hygrometric conditions of an archaeological site affected by unlike boundary weather conditions. Build. Environ. 2014, 76, 125– 133.
16. García, H. Descartan la Pirámide de Cristal de la Almoina por el Efecto Sauna en el Museo. Available online: https://www.levante- emv.com/valencia/2013/06/05/descartan-piramide-cristal-almoina-efecto- 12891562.html (accessed on 08 April 2022).
17. Çetin, F.Y.; İpekoğlu, B. Impact of transparency in the design of protective structures for conservation of archaeological remains. J. Cult. Herit. 2013, 14, e21– e24.
18. Michalski, S. Damage to museum objects by visible radiation (Light) and ultraviolet radiation (UV). In Proceedings of the Lighting in Museums, Galleries and Historic Houses, Bristol, UK, 9–10 April 1987; Papers of the Conference; pp. 3–16.
19. Michalski, S. The Lighting Decision. In Fabric of an Exhibition, Preprints of Textile Symposium 97; Canadian Conservation Institute: Ottawa, ON, Canada, 1997, pp. 97-104.
20. Horie, C.V. Solar control films for reducing light levels in buildings with daylight. Stud. Conserv. 1980, 25, 49–54.
21. Al-Obaidi, K.M.; Ismail, M.; Abdul Rahman, A.M. A review of skylight glazing materials in architectural designs for a better indoor environment. Mod. Appl. Sci. 2014, 8, 68.
22. Parisi, A. Quantitative evaluation of the personal erythemal ultraviolet exposure in a car. Photodermatol. Photoimmunol. Photomed. 1998, 14, 12–16.
23. Kimlin, M.G.; Parisi, A. Ultraviolet radiation penetrating vehicle glass: A field based comparative study. Phys. Med. Biol. 1999, 44, 917–926.
24. Kimlin, M.G.; Parisi, A.; Carter, B.; Turnbull, D. Comparison of the solar spectral ultraviolet irradiance in motor vehicles with windows in an open and closed position. Int. J. Biometeorol. 2002, 46, 150–156.
25. Tuchinda, C.; Srivannaboon, S.; Lim, H.W. Photoprotection by window glass, automobile glass, and sunglasses. J. Am. Acad. Dermatol. 2006, 54, 845–854.
26. Li, D.; Li, Z.; Zheng, Y.; Liu, C.; Lu, L. Optical performance of single and double glazing units in the wavelength 337–900 nm. Sol. Energy 2015, 122, 1091–1099.
27. Serrano, M.A.; Moreno, J.C. Spectral transmission of solar radiation by plastic and glass materials. J. Photochem. Photobiol. B Biol. 2020, 208, 111894.
28. Fernández-Rojas, F.; Fernández-Rojas, C.; Salas, K.J.; García, V.J.; Marinero, E. Conductividad térmica en metales, semiconductores, dieléctricos y materiales amorfos. Rev. Fac. Ing. UCV Caracas 2008, 23, 5–15.
29. Long, L.; Ye, H.; Zhang, H.; Gao, Y. Performance demonstration and simulation of thermochromic double glazing in building applications. Sol. Energy 2015, 120, 55– 64, doi:10.1016/j.solener.2015.07.025; ISSN 0038-092X.
30. Aguilar, J.O.; Xamán, J.; Olazo-Gómez, Y.; Hernández-López, I.; Becerra, G.; Jaramillo, O.A. Thermal performance of a room with a double glazing window using glazing available in Mexican market. Appl. Therm. Eng. 2017, 119, 505–515, doi:10.1016/j.applthermaleng.2017.03.083; ISSN 1359-4311.
31. International Commission on illumination CIE DIS 017/E:2016 ILV: International Lighting Vocabulary. Available online: https://cie.co.at/e-ilv (accessed on 08 April 2022).
32. CEN/TS 16163:2014 Conservation of Cultural Heritage. Guidelines and Procedures for Choosing Appropriate Lighting for Indoor Exhibitions. Available online: https://standards.cen.eu/dyn/www/f?p=204:110:0::::FSP_PROJECT:34047&cs=1AFCAEA358660F36ECF4D92D51A8AD2FC (accessed on 08 April 2022).
33. Tukey, J.W. (1980). We need both exploratory an confirmatory. American Statistician, 34, pp.23-35.
34. Croxton, F.E. (1953), Elementary statistics with applications in medicine and the biological sciences. Dover Pubns.
35. Gifford, E.W., Kroeber, A.L. (1937). Culture element distributions: IV, Pomo. University of California. Publications in American Archaeology and Ethnology, 37, pp.117-255.
36. Kluckhohn, C. (1939). On certain recent applications of association coefficients to ethnological data. American Anthropologist, 41, pp. 345-377.
37. Milke, W. (1935). Sudostmelanesien, eine ethnostatistiche Analyse. Wurzburgo.
38. Driver, H.E. (1961). Introduction to statistics for comparative research. Publicado en Moore, F.W. ed. Readings in cross-cultural methodology. Hraf Press, New Haven, pp. 303-331.
39. Serrano, M.-A.; Baró Zarzo, J.-L.; Moreno Esteve, J.-C.; García-Diego, F.-J. Spectral Relative Attenuation of Solar Radiation through a Skylight Focused on Preventive Conservation: Museo de L'almoina in Valencia (Spain) Case Study. Sensors (2021), 21, 4651. https://doi.org/10.3390/s21144651
40. Ocean Optics, Spectrometers. Available online: https://www.oceaninsight.com/products/spectrometers/ (accessed on 29 July 2021).
41. Reworked from Ocean's diagram. Available online: https://www.oceaninsight.com/products/spectrometers/ (accessed on 29 July 2021).
42. Ocean Insight. Available online: https://www.oceaninsight.com/products/spectrometers/ (accessed on 29 July 2021).
43. Wolf, E. Principios de Óptica. (1999) ISBN-978-O-521-78449-8